Prolonged insula activation during perception of aftertaste

George Andrew James[a], Xuebing Li[c], Grant E. DuBois[b], Lei Zhou[a] and Xiaoping P. Hu[a]

Although a critical component of taste perception, the neural basis of aftertaste perception has yet to be elucidated with neuroimaging. This functional neuroimaging study assessed the temporal dynamics of neural responses to sucrose and aspartame in eight healthy volunteers. Aspartame has a sweetness flavor profile similar to sucrose but a longer temporal profile. Participants underwent functional magnetic resonance imaging while tasting sucrose and aspartame solutions administered through a magnetic resonance imaging compatible delivery device. The insula showed significantly longer activation to aspartame than sucrose, whereas other regions activated by the task (somatosensory cortex, thalamus, amygdala, and basal ganglia) did not show a prolonged response to either tastant. These findings implicate the insula in aftertaste perception. ***NeuroReport***

20:245–250 © 2009 Wolters Kluwer Health | Lippincott Williams & Wilkins.

NeuroReport 2009, **20:**245–250

Keywords: aftertaste, aspartame, experimental design, functional magnetic resonance imaging, sucrose, taste

[a]Department of Biomedical Engineering, Biomedical Imaging Technology Center, Emory University/Georgia Institute of Technology, [b]Corporate Research, The Coca-Cola Company, Atlanta, Georgia, USA and [c]Key Laboratory of Mental Health, Chinese Academy of Sciences, Beijing, China

Correspondence to George Andrew James, 531 Asbury Circle, Suite N305, Atlanta, Georgia 30322-4600, USA
Tel: +1 404 712 2696; fax: +1 404 712 2707; e-mail: ajames@bme.emory.edu

Received 26 September 2008 **accepted** 9 October 2008

Introduction

Spurred by growing worldwide prevalence of obesity [1,2], noncaloric sweeteners are increasingly sought by food manufacturers and consumers alike as substitutes to sucrose. Despite the commercial development of numerous noncaloric sweeteners [3,4], and whereas some (e.g. aspartame and sucralose) are comparable in flavor profile (i.e. relative intensities of sweet, sour, salty, and bitter taste attributes), adequate reproduction of the temporal profile (i.e. change in sweetness intensity over time) of sucrose remains a challenge [5]. Most noncaloric sweeteners are perceived as having a prolonged temporal profile (i.e. sweetness linger or sweet aftertaste) than their natural carbohydrate counterparts, which frequently reduces their palatability.

The development of improved noncaloric sweeteners may benefit by elucidating the relationship between a sweetener's temporal profile and its elicited neural activity. An earlier neuroimaging work has addressed the immediate neural response to taste perception, which includes activation of the insula, orbitofrontal cortex, and amygdala [6–9]. As the primary taste cortex, the insula (and adjacent operculum) is critical for identifying taste components independent of stimulus reward value [10]. The spatial extent of the insular response to tastant (e.g. sucrose) is consistent within-subject but variable across-subject [11]. Both amygdala and orbitofrontal cortex encode stimulus value [12]. Although these regions have overlapping function, the amygdala is associated more with encoding intrinsic stimulus reward value, such as the emotional intensity of affective pictures [13] or an individual's preference for a specific food [14]. The amygdala has also been suggested to assess stimulus relevance [15]. Conversely, orbitofrontal activity is more associated with extrinsic or situational stimulus reward value, perhaps best demonstrated by the variation in orbitofrontal response with eating chocolate to satiety [16] or conditional stimulus valence [17].

Neuroimaging investigations to date have focused on the immediate neural response to tastants – and as such, cannot address tastant aftertaste, an important aspect of taste perception. Aftertaste duration has critical implications for fast event-related functional magnetic resonance imaging (fMRI) studies. For fMRI, the blood oxygen level-dependent (BOLD) response to a stimulus peaks around 4 s and returns to baseline around 12 s poststimulus [18]. The mathematical deconvolution of the stimulus BOLD response in a fast event-related fMRI paradigm assumes that all stimuli elicit responses of equal duration. A violation of this assumption would manifest as a comingling of one stimulus response into the next, which could severely confound the interpretation of results. This violation is best avoided by explicitly modeling the BOLD response duration for individual stimuli or by optimizing the event-related paradigm with increasing the time between trials; both of these modifications work best when incorporated into the paradigm design *ad hoc*.

A slow event-related design was used to assess the temporal profiles of the neural response to a natural carbohydrate and a synthetic noncaloric sweetener.

0959-4965 © 2009 Wolters Kluwer Health | Lippincott Williams & Wilkins DOI: 10.1097/WNR.0b013e32831d2441

Sucrose and aspartame were used as the natural carbohydrate and the synthetic noncaloric sweeteners, respectively, given their similar sweetness flavor profiles but considerably different aftertaste durations. Any prolonged neural activations are anticipated to occur in the insula; as this region primarily processes interoceptive stimuli, it should be activated by both taste and after taste sensation. Conversely, activity in the regions mediating reward (amygdala and orbitofrontal cortex) is not anticipated to persist, as the initial taste sensation is expected to be more rewarding than aftertaste.

Methods

Apparatus

We developed a solution delivery device for use in conjunction with fMRI scanning. Our device resembles a previously proposed device despite its independent design [6]. The device consisted of two units: a control unit kept within the control room and a delivery unit kept within the scanner room. The control unit was composed of a NI PCI-6704 analog output device (National Instruments Peaks) attached to a Dell OptiPlex 170L computer (3 GHz processor, 1 GHz RAM; Dell USA Corporation, Round Rock, Texas, USA). In-house programs written in LabView 8.0 (National Instruments Peak) used the analog output device to operate a CC1116-ND relay array (Digi-Key Corporation; Thief River Falls, Minnesota, USA) of eight four-way solenoid control valves (Acro Associates, Concord, California, USA).

The delivery unit was composed of an eight-channel perfusion pressure kit connected to a bank of eight 50-ml plastic syringes (Automate Scientific, San Francisco, California, USA). Plastic tubing fed compressed air from the scanner room into the top of each syringe to keep the solutions within superfused. Tubing from each syringe tip passed through a nonmagnetic pneumatic pinch valve in the default closed position (Acro Associates Peak) before ending in the participant's mouth. The eight pneumatic pinch valves were opened and closed by compressed air fed from the scanner room through the eight solenoid control valves. These valves, operated through lab view, controlled the flow of air that opened and closed the pinch valves, thus independently controlling solution delivery for each syringe.

Procedures

Neuroimaging was performed on a MAGNETOM Trio 3T Tim system (Siemens Medical Solutions, Malvern, Pennsylvania, USA) with their 12-channel MATRIX imaging head coil. Participants lied supine with the stimulus supply tubing resting on the tip of their tongues. Foam padding restricted head motion. Participants underwent a 5-min MPRAGE image for acquisition of high-resolution anatomy (sagittal slices, resolution = $1 \times 1 \times 1\,mm^3$, field of viewm, $176 \times 224 \times 256$ mm) followed by five 10-min long echo-planar imaging scans. A Z-SAGA scanning sequence was used to reduce artifactual ablation of orbitofrontal cortex and amygdala [19]. Scanning parameters were repetition time = 2000 ms, echo time 1/echo time 2 = 30/68 ms, matrix = $64 \times 64 \times 20$, field of view, $220 \times 200 \times 60$ mm; resolution = $3.44 \times 3.44 \times 4.00\,mm^3$. Each functional scan consisted of five 2-min long blocks with the stimulus events shown in Table 1. The order of stimulus delivery blocks was either S-A-W-A-S or A-S-W-S-A (S = sucrose, A = aspartame, W = water), with counterbalancing across functional scans. Solutions were superfused at 5 PSI to attain delivery of approximately 5 ml of solution per 2-s delivery period (about 2.5 ml/s).

Solution preparation

Solutions were freshly prepared before each scanning session. The rinse solution was a mineral solution (400 mg/l NaCl, 496 mg/l KCl, 500 mg/l KH_2PO_4, dissolved in distilled water and titrated to pH 7 with 0.25N NaOH) to approximate the mineral composition of saliva. The sucrose solution was 8% weight per volume sucrose dissolved in rinse solution. The aspartame solution was 400 mg/l aspartame dissolved in rinse solution.

Participants

Thirteen participants [nine men, mean (SD) age = 30 (6.7) years] were recruited for this study in accordance with Emory University Institutional Review Board policy. Participants provided written consent to involve in this study and were provided monetary compensation. Technical error prevented the scanning of one participant. Neuroimaging data from four participants could not be used because of excessive head motion from

Table 1 Timing of events within each stimulus block

Time since block onset (s)	Participant sees	Participant action	GLM condition
1–10	Juice is coming	Prepares for juice delivery (sucrose, aspartame, or rinse)	Instruction
10–12	Juice delivery	Holds juice in mouth	Delivery_sucrose
12–16	Taste	Tastes juice in mouth	Delivery_aspartame or delivery_rinse
16–18	Swallow	Swallows juice	Peak_sucrose,
18–30	+	Completes swallowing; views fixation; waits for next cue	Peak_aspartame or Peak_rinse
30–90	+	Views fixation; waits for next cue	Baseline_sucrose, baseline_aspartame or baseline_rinse
91–100	Juice is coming	Prepares for juice delivery (always rinse only)	Instruction
100–102	Juice delivery	Holds juice in mouth	Delivery_rinse
102–106	Taste	Tastes juice in mouth	
106–108	Swallow	Swallows juice	Peak_rinse
108–120	+	Completes swallowing; views fixation; waits for next cue	

GLM, general linear model.

swallowing. All neuroimaging results reported are for this reduced sample [six men, mean (SD) age = 29 (4.3) years].

Data processing

All data processing was performed with AFNI [20]. Functional datasets underwent slice timing correction, motion correction, bandpass temporal filtering (0.008–0.08 Hz) without linear detrending, scaling to percent signal change from mean baseline, and spatial smoothing (Gaussian kernel = 5 mm full-width at half-maximum). Neural responses to the experimental manipulations were modeled for each participant with a fixed-effects general linear model (GLM) implemented with AFNI's 3dDeconvolve. Time points corresponding to the four experimental conditions (Instruction, Delivery, Peak, and Baseline) are shown in Table 1.

Several considerations went into designing this GLM. Of primary importance was establishing a clean baseline condition for each solute without contamination from the act of swallowing. Thus, the 'baseline' condition began 12 s postswallow, to ensure ample time for hemodynamic responses from swallowing to return to baseline. Second, anticipation and/or preparation for delivery could elicit a confounding neural response. Thus, solute delivery and swallowing was separated into an early 'delivery' condition (10–16 s) and a later 'peak' condition (16–30 s). These two conditions cannot be statistically deconvolved, as delivery always precedes peak. The 4–6 s delay in onset of peak hemodynamic responses, however, means that the BOLD response to solute tasting should be greatest during the peak GLM condition.

The contrasts peak_sucrose versus baseline_rinse and peak_aspartame versus baseline_rinse yielded widespread insular activation. Spatial activations for these contrasts were consistent within-subject but variable across-subject. The peak_sucrose versus baseline_rinse contrast was thus used to generate a manually defined region of interest (ROI) mask for each participant. Multiple 4-mm radius spheres were centered atop peak activations by participant for the following ROIs: insula, basal ganglia, amygdala, somatosensory cortex, and thalamus. ROI timecourses were extracted using AFNI's 3dMaskave, scaled by setting the 4th timepoint of each block to zero, then averaged across blocks to generate mean timecourses by participant and/or solute condition (sucrose, aspartame).

Results

The location of activation foci varied across participants, prompting individual GLM analysis. Sucrose and aspartame elicited robust bilateral activation of the insula, amygdala, thalamus, and somatosensory cortex, demonstrated for one participant (Fig. 1). Some individuals also demonstrated basal ganglia activation, but this response was less consistent across participants than activations in other regions (i.e. insula).

Figure 2 shows activation timecourses for these regions' responses to each tastant. Both sucrose and aspartame elicit a peak change in BOLD signal of approximately 1% for insula, amygdala, and somatosensory cortex. The peak thalamic response was approximately 0.8% (not shown), whereas the basal ganglia response was approximately 0.3–0.5%. Multivariate analysis of variance

Fig. 1

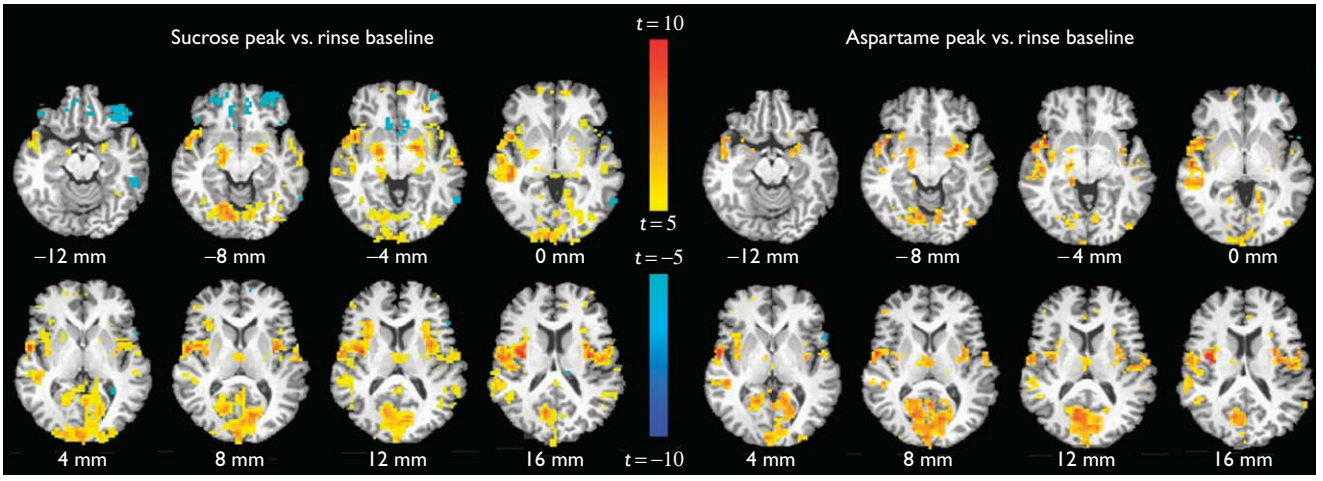

Neural activation after delivery of sucrose (left) and aspartame (right). Results depict results of a voxel-wise general linear model contrast between peak_sucrose or peak_aspartame (left and right, respectively) and baseline_rinse conditions described in Table 1. Insular activation varied considerably across subjects, so results are shown for a single participant. Activation maps are thresholded at $|t|>5$, uncorrected. Color coding is as follows: blue, $t<-5$; yellow, $t>5$; orange, $t>7$; and red, $t>10$.

Fig. 2

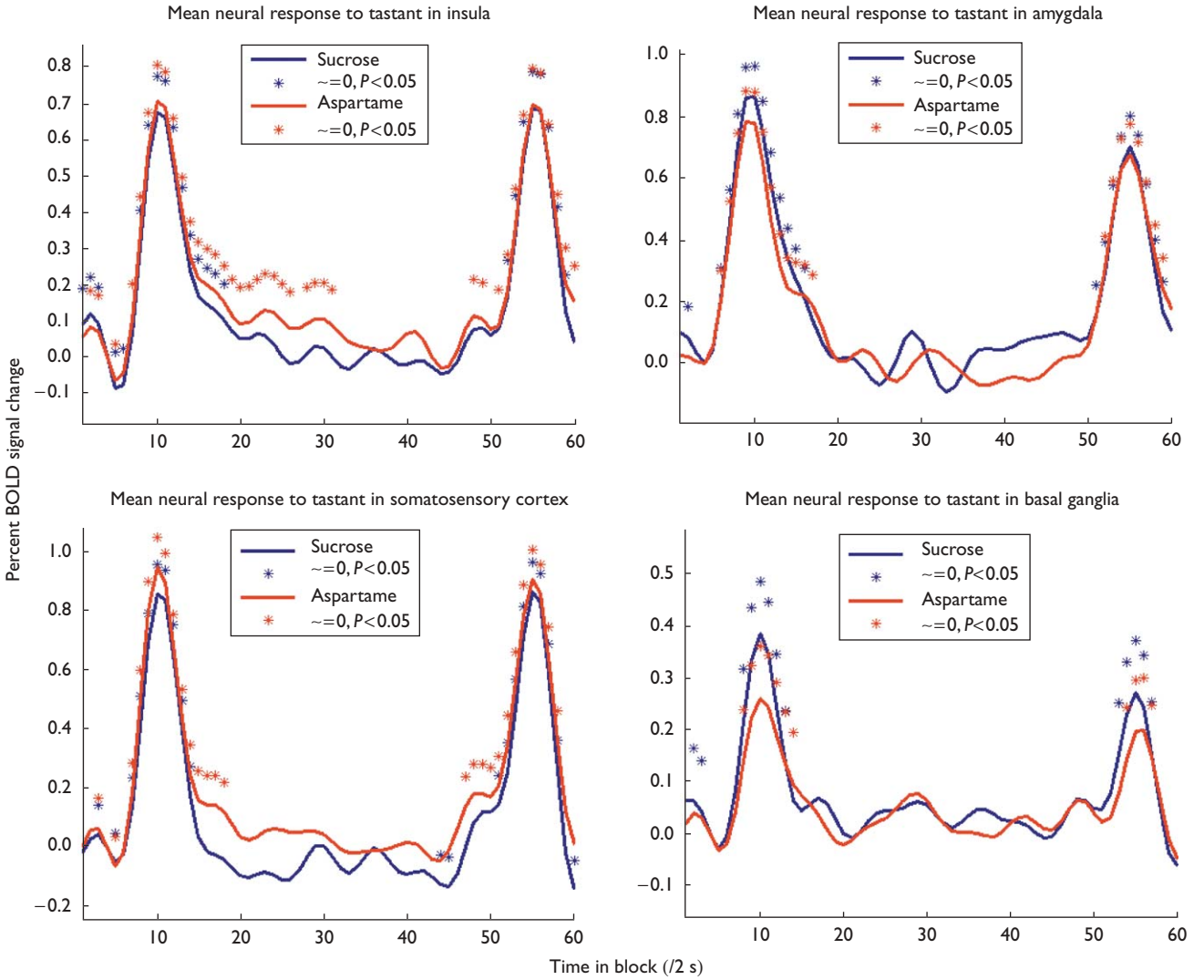

Mean activation timecourses for sucrose and aspartame by region of interest. Each curve is the mean of all participants' activations timecourses for all sucrose (blue) or aspartame (red) blocks. *Timepoints for which mean activation significantly differs from zero (*z* test, $P<0.05$). Note: delivery of stimulus solution (sucrose, aspartame, or rinse) and rinse occur at timepoints 5 and 50, respectively.

assessed the influence of factors ROI and tastant on BOLD signal at timepoints 10 and 23 (10 and 26 s posttastant delivery, respectively).

At timepoint 10, only the main effect of ROI was significant [$F(5,1199) = 23.21$, $P < 0.001$]. Insula, amygdala, thalamus, and somatosensory cortex had the greatest mean BOLD response (0.65, 0.78, 0.65, and 0.88%, respectively), whereas basal ganglia and hippocampus had the smallest response (0.33 and 0.27%). Mean activity for all of the ROIs significant differed from zero ($P < 0.05$). At timepoint 23, the interaction between ROI and stimulus had a trend toward significance [$F(10,1999) = 1.65$, $P = 0.09$]. For this timepoint, the mean insula activity significantly differs from zero only for the aspartame condition ($P < 0.05$); no other ROIs and solutes combination significantly differs from zero. Additionally, the insula's mean response to aspartame remains a full standard deviation above its response to sucrose for timepoints 24–33.

Graphical depiction makes this difference readily apparent. For all regions, the neural response to sucrose returned to baseline within 8–18 s after swallowing the tastant. Insular response to aspartame, however, remained significantly elevated above baseline for 42 s postswallow – over twice as long as the insular response to sucrose. This prolonged response to aspartame was unique to the insula; the neural response of all other regions to aspartame returned to

baseline within 20 s of swallowing. Furthermore, the insular response to sucrose and aspartame was consistent across scan runs.

Discussion

This is the first neuroimaging study to report a neural response to the perception of aftertaste. We sought to find regions that responded identically to both sucrose and aspartame (given their similar sweetness profiles) but with a prolonged response to aspartame (given aspartame's longer aftertaste than sucrose). The insula showed this pattern of activation. A prolonged activation to aspartame was only observed in the insula; the somatosensory cortex, amygdala, basal ganglia, and thalamus all showed a peak response that quickly extinguished postswallow. Likewise, the neural responses of all regions to sucrose similarly extinguished postswallow.

We were unable to resolve insular activation to a single peak. To capture the neural response posttastant, we needed a relatively long interstimulus interval (60 s), which, in turn, constrained the number of trials ($n = 25$ total, with 2 min/trial) and prompted the use of relatively liberal GLM statistical threshold ($|t| > 5$, uncorrected). An independent components analysis could not separate the insular peaks into separate components, showing the peaks to be temporally synchronized. Some of the insular peaks may reflect taste perception while others reflect additional interoceptive processing (i.e. swallowing); however, the contrast peak_sucrose versus peak_rinse yielded comparable insular activations as the peak_sucrose versus baseline_rinse contrast. Given these findings, we do not consider a broad insula ROI to be inherently suboptimal. If anything, a broad ROI is diluting our signal with noise; yet we still find significant differences in the insular responses to tastant aftertaste.

The insula's involvement in aftertaste perception is not surprising. An extensive neuroimaging literature implicates the insula in taste perception [7]. These results are intriguing because they address the neurobiology underlying persistent taste stimulation. Drawing analogy to the tactile sensory system, some receptors respond to changes in stimulation (e.g. Pacinian corpsules), whereas other receptors respond throughout the duration of stimulation (e.g. Merkel nerve endings, nociceptors) [21]. This mechanism of sensory gating allows attentional resources to focus more succinctly upon situationally relevant stimuli. The prolonged activation of the insula to aftertaste implicates tastes as belonging to the latter set of stimuli – that is, stimuli always demanding attentional resources. This heightened relevance of aftertaste stimuli characterizes its evolutionary importance for survivability.

As discussed above, the insula and amygdala have previously been implicated in taste processing. We did not find activation of the orbitofrontal cortex, despite usage of a scanning sequence to reduce signal loss from this region because of proximity of the sinus cavities [19]. One explanation may be the novelty of the sucrose and aspartame solutions. Perhaps familiar tastants would encourage goal-directed taste associations – and corresponding orbitofrontal activity. The somatosensory cortex activation is likely corresponds to movement of the mouth and tongue during tasting and swallowing of stimuli [22]. The basal ganglia aid the amygdala with processing the intrinsic reward value of stimuli, tastant or otherwise [23,24]. Finally, the thalamus is a critical component for integrating sensory information – here, the tactile and chemosensory components of the stimuli [25].

The observed changes in BOLD response are relative small (approximately 1%). Our reduced power is likely results from having relatively a few trials coupled with the lengthy baseline necessary to detect aftertaste responses. An optimized paradigm for detecting differences in tastant quality would yield more robust changes in BOLD, but at the expense of quantifying differences in aftertaste perception [6]. We also report considerable intersubject differences in basal ganglia activation to stimuli. The basal ganglia are highly involved in reward processing. Posttastant manual judgments of taste valence could have elucidated the relationship between basal ganglia activity and taste preference. This study, however, specifically excluded such judgments as they might have obscured the aftertaste response we sought. Interestingly, insular responses were consistent across-subjects, suggesting the insula is nonsubjectively appraising taste profile rather than taste preference.

Insular response was consistent across repeated tastant trials. Peak neural response did not significantly change between the first and last scan. The return to baseline was likewise consistent. These results further show the robustness of the neural response to natural carbohydrate and synthetic noncaloric sweeteners, despite repeated exposures and lengthy scan times. In conclusion, we have demonstrated a neural response specific to aftertaste perception, using a device and paradigm feasible for future studies of tastants.

Conclusion

We report a prolonged neural activation to tastant corresponding to the prolonged aftertaste of the synthetic noncaloric sweetener aspartame. The prolonged activation was specific to the primary taste cortex (insula) and was not observed for other regions, including somatosensory cortex and those mediating reward (amygdala). This persistent neural activation reinforces the evolutionary importance of taste perception for survivability. The extended neural response to aspartame poses a potential methodological confound for future fast event-related neuroimaging studies investigating sweetener palatability.

Acknowledgements

This research was supported by funding from The Coca-Cola Company and NIBIB Grant RO1EB002009. Dr Grant DuBois is an employee of the funding agency, The Coca-Cola Company. To avoid conflict of interest, Dr DuBois assisted with manuscript preparation and experimental design but was not involved in data acquisition or interpretation of results. All other authors report no conflict of interest. This study was conducted at Emory University, Atlanta, Georgia, USA.

References

1 Walker AR, Wadee A. World-wide rises in obesity: minimal hopes of control. *J R Soc Health* 2006; **126**:16–17.
2 Wang Y, Lobstein T. World-wide trends in childhood overweight and obesity. *Int J Pediatr Obes* 2006; **1**:11–25.
3 Kant R. Sweet proteins–potential replacement for artificial low calorie sweeteners. *Nutr J* 2005; **4**:5.
4 St-Onge MP, Heymsfield SB. Usefulness of artificial sweeteners for body weight control. *Nutr Rev* 2003; **61**:219–221.
5 Dubois GE, Lee JF. A simple technique for the evaluation of temporal taste properties. *Chem Senses* 1983; **7**:237–247.
6 Haase L, Cerf-Ducastel B, Buracas G, Murphy C. On-line psychophysial data acquisition and event-related fMRI protocol optimized for the investigation of brain activation in response to gustatory stimuli. *J Neurosci Methods* 2006; **159**:98–107.
7 Small DM, Zald DH, Jones-Gotman M, Zatorre RJ, Pardo JV, Frey S, *et al.* Human cortical gustatory areas: A review of functional neuroimaging data. *Neuroreport* 1999; **10**:7–14.
8 Simmons WK, Martin A, Barsalou LW. Pictures of appetizing foods active gustatory cortices for taste and reward. *Cerebr Cortex* 2005; **15**:1602–1608.
9 Small DM, Gregory MD, Mak YE, Gitelman D, Mesulam MM, Parrish T. Dissociation of neural representations of intensity and affective valuation in human gestation. *Neuron* 2003; **39**:701–711.
10 Sander D, Grafman J, Zalla T. The human amygdala: an evolved system for relevance detection. *Rev Neurosci* 2003; **14**:303–316.
11 Schoenfeld M, Neuer G, Tempelmann C, Schubler K, Noesselt T, Hopf J-M, *et al*. Functional magnetic resonance tomography correlates of taste perception in the human primary taste cortex. *Neuroscience* 2004; **127**:347–353.
12 Gottfried JA, O'Doherty J, Dolan RJ. Encoding predictive reward value in human amygdala and orbitofrontal cortex. *Science,* 2003; **301**:1104–1107.
13 Phan KL, Taylor SF, Welsh RC, Ho SH, Britton JC, Liberzon I. Neural correlates of individual ratings of emotional salience: a trial-related fMRI study. *Neuroimage* 2004; **21**:768–780.
14 Hinton EC, Holland AJ, Gellatly MS, Soni S, Owen AM. An investigation into food preferences and the neural basis of food-related incentive motivation in Prader-Willi syndrome. *J Intellect Disabil Res* 2006; **50**:633–642.
15 Wedig MM, Rauch SL, Albert MS, Wright CI. Differential amygdala habituation to neutral faces in young and elderly adults. *Neurosci Lett* 2005; **385**:114–119.
16 Small DM, Zatorre RJ, Dagher A, Evans AC, Jones-Gotman M. Changes in brain activity related to eating chocolate: from pleasure to aversion. *Brain* 2001; **124**:1720–1733.
17 Cox SM, Andrade A, Johnsrude IS. Learning to like: a role for human orbitofrontal cortex in conditioned reward. *J Neurosci* 2005; **25**:2733–2740.
18 Aguirre GK, Zarahn E, D'Esposito M. The variability of human, BOLD hemodynamic responses. *Neuroimage* 1998; **8**:360–369.
19 Heberlein KA, Hu X. Simultaneous acquisition of gradient-echo and asymmetric spin-echo for single-shot z-shim: Z-SAGA. *Magn Reson Med* 2004; **51**:212–216.
20 Cox RW. AFNI: software for analysis and visualization of functional magnetic resonance neuroimages. *Comput Biomed Res Int J* 1996; **29**:162–173.
21 Johnson KO, Yoshioka T, Vega-Bermudez F. Tactile functions of mechanoreceptive afferents innervating the hand. *J Clin Neurophysiol* 2000; **17**:539–558.
22 Penfield W. The cerebral cortex in man: 1. The cerebral cortex and consciousness. *Arch Neurol Psychiatr* 1938; **40**:417–442.
23 Delgado M. Reward-related responses in the human striatum. *Ann N Y Acad Sci* 2007; **1104**:70–88.
24 Knutson B, Cooper J. Functional magnetic resonance imaging of reward prediction. *Curr Opin Neurol* 2005; **18**:411–417.
25 Katz D, Nicholelis M, Simon S. Gustatory processing is dynamic and distributed. *Curr Opin Neurobiol* 2002; **12**:448–454.